DESIGN, SYNTHESIS AND REACTIVITY OF NOVEL TRANSITION METAL COMPLEXES OF 1,3-DIKETONATES BEARING PERFLUORINATED OR HETEROCYCLIC MOIETIES

Jo' Del Gobbo

Instituto Superior Técnico, Universidade de Lisboa

December/2022

Abstract. β-Diketonate ligands hold an important place in the history of coordination chemistry and continue to be among the most ubiquitous ligands. The most unique feature is their ability to coordinate most of all known elements. The first part of the research project has been mainly focused on the syntheses of a sterically hindered β-diketonate, 1,3-dimesitylpropane-1,3-dione (HL^{Mes}) and of a further sterically hindered β-diketonate ligand, bearing fluorinated moieties, the 1,3-bis(3,5-bis(trifluoromethyl)phenyl)-3-hydroxyprop-2-en-1-one (HL^{CF3}). Their reactivity has been investigated through the synthesis of the related Zn(II), Cu(II), Cu(I) and Ag(I) complexes. The second part has concerned the development of a platform for the synthesis of new N,O,O-donor chelating species as a new class of "scorpionate" ligands, based on the 3-benzylidene-2,4-pentanedione skeletal functionalized with heterocyclic rings. In particular, the 3-(phenyl(1H-pyrazol-1-yl)methyl)pentane-2,4-dione (HL^{J}), a novel 1,3-diketonate bearing a pyrazole moiety (whose reactivity and structure have been fully studied also by X-ray diffraction analysis), and the 1-(3,5-dimethyl-1H-pyrazol-1-yl)-3-phenylpropane-1,3-dione (HL^{JM}) containing a pyrazole unit functionalized in 3- and 5-position. Each ligand has been used to synthesize different types of metal complexes by using Zn(II), Cu(II), Cu(I) and Ag(I) acceptors with the aim to investigate the chemical properties (reactivity, stability, geometry) of the new ligands and related complexes. In the syntheses of Cu(I) and Ag(I) complexes, a phosphane coligand, such as triphenylphosphine was also used to stabilize silver and copper in +1 oxidation state. Biological studies to evaluate the antitumor and antiviral activity are in progress for some of the ligands and related metal complexes.

Keywords: β-diketones, sterically hindered β-diketonates, N,O,O-donor chelating species, transition metal-based complexes, phosphanes, X-ray analysis.

1. Introduction

Nowadays one of the purposes of chemistry research is the development of base metal catalysts that can compete with precious metals [1-3]. Precious metals, that are relatively non-abundant in Earth's crust and/or difficult to extract, have various economic, scalability, sustainability and toxicity problems [4, 5], but they are indispensable in homogeneous catalysis [6-9]. Further, these metals often rely on expensive ligand classes to support their chemistry. Demand for precious metals has increased over the past few decades, increasing their prices and motivating research into base metal catalysis. Instead, the earth-abundant base metals are economical and generally non-toxic [10, 11]. However, there is a critical need for ligand classes that promote the high-spin reactivity exhibited by the first transition series.

According to Goldschmidt, the base metals are distinguished by their tendency to bond with oxygen or sulfur, and so to form a slag that cooled and became the Earth's crust. β-Diketones, as bidentate ligands through two oxygen atoms, are well suited to coordinate these elements such as copper, lead, nickel, zinc, tin, aluminum. Metal acetylacetonates have been used in catalysis for almost a century, in a variety of important bond forming reactions [12]. Classical β-diketones and related ligands have been studied for more than a century and their ability to give rise to a rich and interesting coordination chemistry is well documented [13]. They act under appropriate conditions as uninegative chelating κ^2-O,O donors, capable of stabilizing mononuclear or polynuclear complexes. β-Diketones exist as an equilibrium mixture of keto and enol tautomeric forms studied in solution by IR and NMR spectroscopy and in the solid state by X-ray single crystal diffraction [14-16]. Generally, the enol tautomer is more stable than the keto tautomer, due to intramolecular H-bonding and simultaneous conjugation [15]. Replacement of electron-withdrawing groups shifts the equilibrium in favor of the enolic form and the reverse happens with electron-releasing substituents. The enolic form is favored in non-polar solvents [17]. Substitutions at the carbon atoms in the chelate ring modify the steric and electronic profile of the

ligand, in turn affecting coordination properties and chemistry. Common modifications include the use of fluorinated, bulky, and/or conjugated side groups. The enolic tautomer of β-diketones has served as a model for intramolecular hydrogen bonding for over a century. The enolic hydrogen can be replaced with a metal atom by sufficiently strong bases or Lewis acidic metals. β-Diketones form six-membered heterocycles with cations having at least two open coordination sites, usually metals but also some non-metals such as for example boron. The bidentate ligands exhibit the "chelate effect", where the coordination is more effective than equivalent monodentate ligands because their dissociation is a multi-step process [18].

The importance of β-diketones in medicinal chemistry lies in the fact that they can be intermediates in the synthesis of COX-2 inhibitors, a type of nonsteroidal anti-inflammatory drugs (NSAIDs). Furthermore, β-diketone moiety can be present in natural products such as curcuminoids, which are known for their antibacterial, neuroprotective and anticancer properties. Complexes of these ligands can also act as phosphors for lighting and high efficiency electroluminescent devices for light-emitting diodes, contrast agents for medical magnetic resonance imaging, transport carriers of alkali metal ions across biological membranes, luminescent probes for proteins and amino acids [19]. Another primary field of interest is the application of metal β-diketonates as liquid crystal phases; because of their special magnetic and electronic properties, these materials are generally known as ''metallomesogens". Most literature in this field is devoted to the β-diketonates of Rh(I), Ir(I), Ni(II), Pd(I), Pt(II), and Cu(II), which have a linear or planar geometry and therefore mimic conventional organic calamitic or discotic liquid crystals [20]. In the field of nanoscale materials, these ligands play an important role as assembly agents in the preparation of high-spin molecules. For example, Fe(III) and Mn(III) clusters containing β-diketonates have shown interesting magnetic anisotropic behavior, also being able to entrap alkaline ions [21].

The β-diketonates provide an exceptionally weak field, ionic interaction with the metal ion, offering a very different electronic environment in comparison with strong-field ligand platforms [22]. While at the same time, the ligand framework is π-acidic and has been described as pseudo-aromatic, speaking to the efficacy of its interaction with ligated metals [23]. Reactions continue to be discovered using base metal β-diketonates, and it is often noted that even modestly sterically hindered ligands offer improvements over the parent acetylacetone [24]. The hindered ligands often contain tert-butyl or iso-propyl substituents, representing the most common "hindered" ligands due to synthetic limitations of the Claisen condensation [25]. The addition of steric bulk to ancillary ligands is a common approach to improving catalyst activity and selectivity, which has yet to be applied to β-diketones. Ligand design is a critical step in synthesizing new and extended inorganic or organometallic structures. Many efforts were made in the last decades of the twentieth century to modify the electronic and steric properties of β-diketones by inserting different substituents, which can also contain additional donor atoms, in order to prepare polyfunctional coordinating ligands as ''biomimetic'' agents with higher complexity and functionality.

2. Experimental section

All reagents used for the synthesis of ligands and complexes were purchased from Sigma-Aldrich and used without further purification. Elemental analyses (C,H,N,S) were performed with a Fisons Instruments EA-1108 CHNS-O Elemental Analyzer (Thermo Scientific). Melting points (M.P.) were taken on an SMP3 Stuart Scientific Instrument. FT-IR spectra were recorded from 4000 to 400 cm^{-1} on a Perkin Elmer Frontier FT-IR instrument, equipped with single reflection ATR unit (universal diamond ATR top-plate) as a sample support. ^{1}H- and ^{31}P-NMR spectra were recorded with a 500 Bruker Ascend (500.1 MHz for ^{1}H and 202,4 MHz for ^{31}P). Referencing is relative to TMS (^{1}H) and 85% H_3PO_4 (^{31}P). ElectroSpray Ionization Mass Spectra (ESI-MS) were obtained in positive- or negative-ion mode on a Series 1100 MSD detector HP spectrometer, using a methanol or acetonitrile mobile phases. The compounds were added to reagent grade methanol or acetonitrile to give approximately 0.1 mM solutions, injected (1 μL) into the spectrometer via a HPLC HP 1090 Series II fitted with an autosampler, at a flow rate of 300 μL/min, employing nitrogen both as drying and nebulizing gas. Capillary voltages were typically 4000 V and 3500 V for the positive- and negative-ion mode, respectively. Confirmation of all major species was aided by comparison of the observed and predicted isotope distribution patterns, the latter calculated using the IsoPro 3.1 computer program.

2.1. Synthesis of the ligands

2.1.1. *Synthesis of* $\mathbf{HL^{CF3}}$ (**1**)

NaH (60% in mineral oil, 11.720 mmol, 0.460 g) was washed with hexane (5 mL) at room temperature under nitrogen atmosphere. Successively, anhydrous THF was added. At the meantime, 3',5'-bis(trifluoromethyl)acetophenone (7.800 mmol, 2.000 g) was combined with methyl 3,5-bis(trifluoromethyl)benzoate (8.580 mmol, 2.320 g) in a separate flask. To this solution, the sodium hydride solution was added dropwise. The resultant mixture was heated at reflux for 36 h. Afterwards, the mixture was cooled at room temperature and a precipitate was formed adding dropwise ice-cold 10% hydrochloric acid (40 mL). The precipitate was dissolved adding diethyl ether (25 mL). The organic layer was then

isolated by extraction, dried over anhydrous Na_2SO_4, filtered and concentrated under vacuum to afford an off-white solid. The solid was recrystallized in acetone to afford the whitish complex in 87% yield.

2.1.2. *Synthesis of* NaL^{CF3} (**2**)

Finely ground NaOH (0.130 g, 3.000 mmol) was added to the ligand HL^{CF3} (1.500 g, 3.000 mmol). The mixture was successively dissolved in ethanol (100 mL), giving an opalescent yellow solution. The reaction was carried out under magnetic stirring at room temperature (r.t.). Through this process the solution slowly assumed a more limpid aspect. After 4 h, the reaction was stopped and the solution was dried at reduced pressure leading to the formation of an orange solid on the bottom of the flask. The solid product was kept into the drier for a night. The solid orange with pale pink reflection was recovered (yield 85%).

2.1.3. *Synthesis of* HL^{Mes} (**3**)

Synthesis of precursor $Al(L^{Mes})_3$: malonyl chloride (13.953 mmol, 1.915 g) was added dropwise to a mixture of mesitylene (33.965 mmol, 4.72 mL) and aluminium trichloride (37.362 mmol, 4.982 g) in carbon sulphide (100 mL) cooled at 0°C. The reaction was stirred at reflux for 24 h. The mixture was then transferred in a round-bottom flask containing HCl (37%, 20 mL), cooled at 0°C. Successively, water (80 mL) was added dropwise, and the mixture was left under constant magnetic stirring for 10 minutes. The organic phase was then separated by the aqueous phase and it was evaporated at reduced pressure giving the whitish $Al(L^{Mes})_3$ in 53% yield. To the complex $Al(^{Mes}acac)_3$ (1.348 mmol, 1.280 g), solubilized in chloroform, concentrated HCl (37%, 10 mL) was added. The reaction mixture was stirred at reflux for 24 h. The aqueous phase was removed and the organic phase was washed with water (3 x 10 mL). The organic phase was anhydrified with sodium sulphate. The mixture was filtered, and the mother liquors were evaporated under reduced pressure to give the whitish brown-orange product HL^{Mes} in 88% yield.

2.1.4. *Synthesis of* $NaL^{Mes}\cdot H_2O$ (**4**)

To the ligand L^{Mes} (308.414 g/mol, 2.838 mmol, 0.875 g) solubilized in MeOH (15 mL), NaOH (2.838 mmol, 0.113 g) was added. The reaction mixture was stirred at reflux for 24 h. The solution was dried at reduced pressure and the residue was recrystallized by diethyl ether and filtered. From the mother liquors, dried at reduced pressure, the light orange whitish complex NaL^{Mes} has been obtained in 74% yield.

2.1.5. *Synthesis of* HL^{J} (**5**)

3-benzylidene-2,4-pentadienone (1.000 g, 5.310 mmol) and an excess of triethylamine (0.628 g, 5.310 mmol) were solubilized in EtOH (20 mL). Successively, pyrazole (0.362 g, 5.310 mmol) was added and a yellow clear solution was observed. The reaction was carried out overnight under magnetic stirring, at r.t. The day after, reflux was applied to the yellow solution for 6 h giving to an intensification of the mixture's colour. During this time, the reaction was monitored by Thin Layer Chromatography. Then, the reflux was removed, and the solution was left under magnetic stirring at room temperature overnight. After 36 h the reaction was controlled by ESI-MS and it was stopped. The mixture was dried at reduced pressure and an orange oil product was observed. The oil was solubilized in Et_2O and precipitated with *n*-hexane until a white precipitate was formed. The white solid product was recovered by filtration (60% yield).

2.1.6. *Synthesis of* HL^{JM} (**6**)

3-benzylidene-2,4-pentanedione (0.011 mol, 2.00 g) and triethylamine (0.011 mol, 1.11 g) were solubilized in EtOH. A clear yellow solution was observed. The reaction was carried out under magnetic stirring, at r.t., for 3 h. Then, 3,5-methylpyrazole (0.011 mmol, 0.96 g) was added. No colour variation was observed. After 24 h the reaction was stopped and the yellow solution was evaporated till dryness, obtainig a colourless oil with yellow reflections. The oil was solubilized with Et_2O and precipitated with *n*-hexane. The white solid formed was filtered and dried (63% yield).

2.2. Synthesis of the complexes

2.2.1. *Synthesis of* $Cu(L^{CF3})_2$ (**7**)

The ligand HL^{CF3} (1.000 mmol, 0.498 g) and $Cu(CH_3CO_2)_2\cdot H_2O$ (0.500 mmol, 0.100 g) were solubilized in H_2O and EtOH (1:1, 20 mL:20 mL). The solution was left under constant magnetic stirring at r.t. for 1 and then at reflux for 4 h. The reaction was stopped, and the precipitate was filtered and dried in air. The whitish complex was obtained in 94% yield.

2.2.2. *Synthesis of* $Cu(PPh_3)_2(L^{CF3})$ (**8**)

$Cu(CH_3CN)_4PF_6$ (0.186 g, 0.500 mmol) and PPh_3 (0.262 g, 1.000 mmol) were solubilized in CH_3CN (40 mL). The reaction mixture was kept under constant magnetic stirring at r.t. overnight. The next day, the ligand NaL^{CF3} (0.260 g, 0.500 mmol) was added to the solution. After 5 h of magnetic stirring, the mixture was evaporated and the solid formed was washed in Et_2O. From the mother liquors an orange solid was precipitated, and it was crystallized using Et_2O and *n*-hexane to give the complex $Cu(PPh_3)_2(L^{CF3})$ in yield 60%.

2.2.3. *Synthesis of* $Zn(L^{CF3})_2$ (**9**)

$Zn(CH_3CO_2)_2$ (0.097 g, 0.500 mmol) and HL^{CF3} (0.524 g, 1.000 mmol) were solubilized in EtOH (15 mL) under magnetic stirring at r.t. Subsequently, H_2O was added to the flask (in a 1 to 1 ratio with EtOH). The mixture was stirred at r.t. overnight. The precipitate formed was washed with $CHCl_3$ and kept for 2 h under magnetic stirring. It was filtered and dried under vacuum to give the $Zn(L^{CF3})_2$ complex in 45% yield.

2.2.4. *Synthesis of* **Ag(PPh$_3$)$_2$(L^{CF3})** (**10**)

$AgNO_3$ (0.085 g, 0.500 mmol) and PPh_3 (0.262 g, 1.000 mmol) were solubilized in MeOH (40 mL). The reaction mixture was stirred for 3 h at r.t., covering the flask with tinfoil. NaL^{CF3} ligand (0.262 g, 0.500 mmol) was added with 10 mL of MeOH and the reaction was carried on for 3 h in the same conditions. The solution was evaporated to dryness and the yellow solid product was solubilized in Et_2O and precipitated in $CHCl_3$. A yellow opalescent mixture with a dark precipitate was formed. The yellow solution was evaporated forming of an orange oil which was dried under reduced pressure. Once dried, it was precipitated with $CHCl_3$ and *n*-hexane. The precipitate was decanted, while the liquid solution was kept in freezer until yellow crystals have formed. The crystals were dried and characterized (yield 65%).

2.2.5. *Synthesis of* **Cu(L^J)$_2$** (**11**)

The ligand HL^J (0,512 g, 2.000 mmol) and $Cu(CH_3CO_2)_2{\cdot}H_2O$ (0.199 g, 1.000 mmol) were dissolved in CH_3OH (40 mL), giving a dark green solution with blue reflex. The reaction proceeded for 12 h at r.t. under magnetic stirring. After this time the mixture becomes opalescent with a blue suspension. At the end the mixture was filtered and the obtained mother liquors were dried at reduced pressure obtaining a blue oil. Et_2O was added into the round bottom flask to purify the residue: a sky-blue precipitate was formed and removed by filtration. The obtained mother liquors were concentrated at reduced pressure and let it evaporate at room temperature. After 2 days at the bottom of the flask a petrol green solid was formed which is recovered. The petrol green complex Cu(L^J)$_2$ was obtained in 58% yield.

2.2.6. *Synthesis of* **[Cu(HL^J)(PPh$_3$)$_2$]PF$_6$** (**12**)

PPh_3 (0.525 g, 2 mmol) and $Cu(CH_3CN)_4PF_6$ (0.372 g, 1 mmol) were dissolved in CH_3CN (40 mL), giving a limpid colorless solution, that is put under magnetic stirring at r.t. for 2 h. After this time, ligand HL^J (0.256 g, 1.000 mmol) was added leaving the solution limpid and colorless. The reaction proceeded over night at room temperature under magnetic stirring. At the end, the solution was dried at reduced pressure giving a yellow oil. Then, using the high vacuum pump a light-yellow precipitate was formed. The light-yellow complex [Cu(L^J)(PPh$_3$)$_2$]PF$_6$ was obtained in 89% yield.

2.2.7. *Synthesis of* **Zn(HL^J)(HPz)Cl$_2$** (**13**)

The ligand HL^J (0.256 g, 1.000 mmol) and $ZnCl_2$ (0.1363 g, 1.000 mmol) were dissolved in EtOH (40 mL), giving a colorless solution. The reaction proceeded for 3 h at r.t. under magnetic stirring. After that the reaction is refluxed for 3 h and then the temperature is lowered to let it proceed at room temperature overnight. At the end, the mixture was dried at reduced pressure giving a yellow oil. The residue was solubilized with anhydrous EtOH and then Et_2O and n-hexane were added into the round-bottom flask in order to purify it: a precipitate was formed, removed by decanting and dried at reduced pressure. The white complex Zn(HL^J)(HPz)Cl$_2$ was obtained in 43% yield.

2.2.8. *Synthesis of* **Cu(L^{Mes})$_2$** (**14**)

The ligand NaL^{Mes} (1.500 mmol, 0.495 g) was solubilized in a mixture of MeOH:EtOH (50:50, 15 mL) and $CuCl_2{\cdot}2H_2O$ (0.750 mmol, 0.128 g) was added. The reaction was left under constant magnetic stirring at r.t. for 24 h. The formation of a precipitate was observed, it was filtered and dried under reduced pressure. The grey-green Cu(L^{Mes})$_2$ complex, was obtained in 68% yield.

2.2.9. *Synthesis of* **Zn(L^{Mes})$_2$** (**15**)

The ligand NaL^{Mes} (1.500 mmol, 0.495 g) was solubilized in absolute EtOH (30 mL) and $ZnCl_2$ was added (0.750 mmol, 0.102 g). The reaction was left under constant magnetic stirring at r.t. for 24 h. The mixture was filtered and the precipitate was dried under reduced pressure. The light yellow complex Zn(L^{Mes})$_2$ was obtained in 50% yield.

3. Results and discussion

3.1. Synthesis and characterization of the ligands

The diketone 1,3-bis(3,5-bis(trifluoromethyl)phenyl)propane-1,3-dione (**HL^{CF3}**) was synthesized in THF solution from a mixture of 3,5-bis(trifluoromethyl)acetophenone and 3,5-bis(trifluoromethyl)benzoate (Scheme 1) by Claisen condensation, using a modified literature method utilized in the synthesis of somewhat related 1,3-bis(4-methylphenyl)propane-1,3-dione [26]. It was isolated as a white solid in 87% yield. The sodium salt **NaL^{CF3}** (**2**) was obtained by dissolving the **HL^{CF3}** (**1**) ligand in an equimolar quantity of NaOH in methanol solution and it was fully characterized. The elemental analysis has confirmed the stoichiometry of the two ligands, showing a good purity of the products.

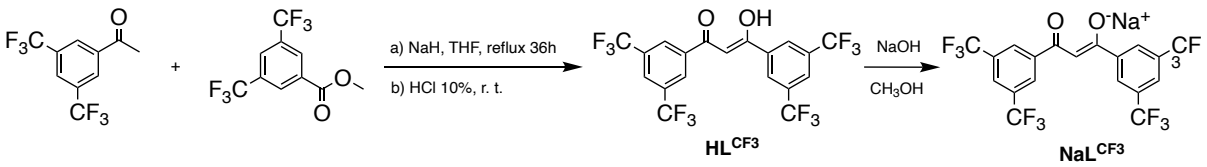

Scheme 1 - Synthetic procedure for the ligands **HL^{CF3}** (**1**) and **NaL^{CF3}** (**2**)

The ^{1}H-NMR spectrum of **HL^{CF3}** in $CDCl_3$ suggests the presence of the enol form, 1,3-bis(3,5-bis(trifluoromethyl)phenyl)-3-hydroxyprop-2-en-1-one, in solution. The 2-C*H* bridging and O*H* protons are detectable at 6.91 and 16.59 ppm, respectively. The C*H* protons in *orto*- and in *para*-positions of aromatic rings are present at 8.46 and 8.13 ppm, respectively. In the ^{13}C-NMR spectrum the 2-*C*H and C=O carbons are detectable at 93.83 and 183.5 ppm, respectively. The ^{19}F-NMR shows only one signal at -63.11 ppm. The IR spectrum of **HL^{CF3}** ligand was carried out on solid sample and it shows all the expected absorption band: weak absorptions at 3099 cm^{-1} due to the C-H bonds; medium absorptions at 1623 and 1576 cm^{-1}, due to the stretching vibrations of the C=O.
The ^{1}H-NMR spectrum of **NaL^{CF3}** was recorded in DMSO solution. It shows a single set of resonances for the two C*H* protons in *orto*- and in *para*-positions of aromatic rings at 8.48 and 8.08 ppm, respectively. The presence of the monoanionic form has furthermore been confirmed by the absence in the spectra recorded in aprotic solvents of the O*H* proton. In addition, in the IR spectrum the stretching vibrations of the C=O groups are shifted at 1628 cm^{-1}.
Following the method used for 1,3-bis(3,5-bis(trifluoromethyl)phenyl)propane-1,3-dione, we attempted to synthesize the 1,3-dimesityl-propane-1,3-dione compound by condensation of 2,4,6-trimethylbenzaldehyde with 2,4,6-trimethylacetophenone. However, the two reactants did not undergo condensation, likely due to the high steric hindrance of the six methyl groups of the two trimethyl-substituted starting materials. As an alternative approach, we have chosen the Friedel-Crafts reaction for the synthesis of **HL^{Mes}** (**3**). The synthesis began from the reaction of malonyl dichloride with mesitylene in the presence of anhydrous aluminum chloride, followed by treatment with HCl/ice (Scheme 2) [27].

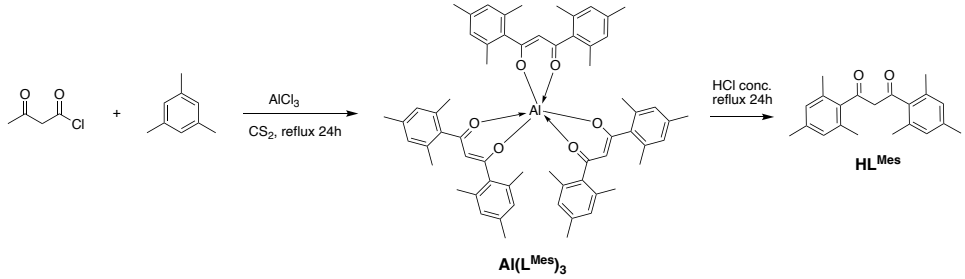

Scheme 2 - Synthesis of 1,3-dimesityl-propane-1,3-dione **HL^{Mes}** (**3**)

The Al(L^{Mes})$_3$ complex was obtained in very high yield and fully characterized. According to literature reports [27, 28], diketones can be obtained by acidification of the intermediate with HCl/ice. Under such mild conditions the Al(III) complex remained intact, probably due to the stability of the complex gained from the six-membered ring chelation together with the ligand steric protection. To promote the dissociation of the Al(L^{Mes})$_3$ complex and the formation of the product, concentrated HCl was used, and the mixture was heated to reflux for 24 h under stirring. The desired 1,3-dimesityl-propane-1,3-dione (**HL^{Mes}**) was then isolated in good yield. The ^{1}H-NMR spectrum of **HL^{Mes}** in $CDCl_3$ shows the characteristic enolic proton absorptions at around 16.04 ppm, the 2-C*H* proton at 5.77 ppm, the -C*H*$_3$ protons in the range 2.32-2.35 ppm and the aromatic meta-C*H* protons at 6.91 ppm. The 2-C*H*$_2$ protons of the keto form are not visible, which is an indication that the enol tautomer is the most dominant form in $CDCl_3$ solvent. The IR spectrum has been carried out on the solid sample of **HL^{Mes}** and it shows all the expected absorption bands. In particular, the band at about 1613 and 1575 cm^{-1} are assigned to the C=O carbonyl groups, and the lower frequency band at 1435 cm^{-1} is due to the C=C double bond. The band at 1270 cm^{-1} can be assigned to the C-O vibration.
The sodium salt **NaL^{Mes}·H$_2$O** (**4**) was obtained by dissolving the **HL^{Mes}** species in an equimolar quantity of NaOH in methanol solution. It was then isolated in high yield. The presence of the monoanionic species has furthermore been confirmed by the absence in the spectra recorded in aprotic solvents of O*H* proton. In addition, in the IR spectrum the stretching vibrations of the C=O groups are shifted at 1611 and 1557 cm^{-1}.
The ligands 3-(phenyl(1*H*-pyrazol-1-yl)methyl)pentane-2,4-dione, **HL^{J}** (**5**), and 3-((3,5-dimethyl-1*H*-pyrazol-1-yl)(phenyl)methyl)pentane-2,4-dione, **HL^{JM}** (**6**), were synthesized in ethanol solution from a mixture of 3-benzylidenepentane-2,4-dione (**L^{A}**) and pyrazole or 3,5-dimethyl-pyrazole under basic conditions for triethylamine (Et_3N) (Scheme 3).

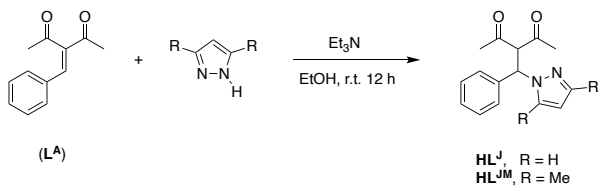

Scheme 3 - Synthetic procedure for the ligands **HL^{J}** (**5**) and **HL^{JM}** (**6**)

Pyrazoles add with surprising ease to the α, β-unsaturated β-dicarbonyl compound 3-benzylidenepentane-2,4-dione. Spontaneous, weakly exothermal reaction affords the new **HL^{J}** and **HL^{JM}** compounds which precipitate from the reaction mixture in very good yield and high purity. The precursor 3-benzylidenepentane-2,4-dione (**L^{A}**) can be synthetized by Knövenagel condensation of an equimolar amount of acetylacetone and benzaldehyde in the presence of piperidine as a catalyst (Scheme 4).

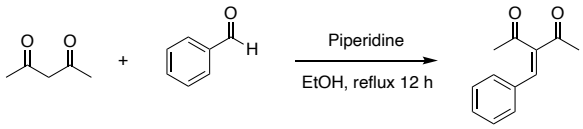

(**L^{A}**)

Scheme 4 - Synthetic procedure for the species **L^{A}**

The elemental analysis has confirmed the stoichiometry of the two ligands **HL^{J}** (**5**) and **HL^{JM}** (**6**), showing a good purity of the products. The ^{1}H-NMR spectra of **HL^{J}** and **HL^{JM}** in $CDCl_3$ suggest the presence of the keto form in solution. In the ^{1}H-NMR spectrum of **HL^{J}**, the 3-C*H* and 4-C*H* protons of pyrazole ring are present at 7.50 and 6.22 ppm, respectively. The 5-C*H* of pyrazole and the C*H* aromatic protons of the phenyl ring are present in the range 7.32-7.41 ppm. The α-*H* and γ-C*H* bridging proton are present at 5.32 ppm (^{3}J = 11.28 Hz) and 6.01 ppm (^{3}J = 11.28 Hz). The singlets at 2.22 and 2.03 ppm are attributable to the methyl groups bonded to the moieties. In the ^{13}C-NMR spectrum the *C*=O, α-*C*H, γ-*C*H and *C*H_3 carbons are detectable at 200.3-200.0, 72.6, 64.2 and 29.9-30.9 ppm, respectively. The 4-*C*H carbon of the pyrazole ring is detectable at 106.10 ppm. In the ^{1}H-NMR spectrum of **HL^{JM}**, the C*H* aromatic protons are present in the range 7.28-7.38 ppm and the α-CH and γ-CH bridging proton are present at 5.82 ppm (^{3}J = 11.11 Hz) and 5.42 ppm (^{3}J = 11.28 Hz). The singlet at 2.21 ppm is attributable to the methyl groups bonded to the β-dicarbonyl moieties. The singlets at 2.00 and 2.18 ppm are attributable to the methyl groups of pyrazole (3-CH_3 and 5-CH_3) and the 4-C*H* proton in the pyrazole ring is present as a singlet at 5.75 ppm. In the ^{13}C-NMR spectrum the *C*=O, α-*C*H, γ-*C*H and *C*H_3 carbons are detectable at 199.9-200.9, 72.4, 60.6 and 30.3-31.6 ppm, respectively. The 4-*C*H carbon of the pyrazole ring is detectable at 105.6 ppm. The ESI-MS study has been performed by dissolving **HL^{J}** and **HL^{JM}** in CH_3CN and CH_3CN, respectively, and recording the spectra in positive- and negative-ion mode. The molecular structure of **HL^{J}** has been confirmed by the presence of the molecular peaks at *m/z* 257 and 279 respectively, attributable to the $[HL^{J} + H]^{+}$ and $[HL^{J} + Na]^{+}$ species. The molecular structure of **HL^{JM}** has been confirmed by the presence of the molecular peaks at *m/z* 285 and 307 respectively, attributable to the $[HL^{JM} + H]^{+}$ and $[HL^{JM} + Na]^{+}$ species. The IR spectra of **HL^{J}** and **HL^{JM}** have been carried out on solid samples and they show all the expected absorption bands. Weak bands in the region 2980-3108 cm^{-1} are assigned to C-H stretching vibrations. The ligands also show two sharp strong bands in the regions 1732-1699 cm^{-1} and 1728-1699 cm^{-l} attributable to the stretching vibrations of the two carbonyl groups. The two bands at *ca.* 1500 cm^{-1} correspond to C=C/C=N rings stretching. Bands in the region 1350-1394 cm^{-1} are assigned to in-plane bending vibrations of the methyl groups. The out-of-plane bending vibrations of the ring C-H bonds are observed in the 776-729 cm^{-1} region.

3.2. Synthesis and characterization of the complexes

The copper(II) complexes $[Cu(L^{CF3})_2]$ (**7**) and $[Cu(L^{Mes})_2]$ (**14**) was synthesized in good yields by dissolving the corresponding ligands **HL^{CF3}** (**1**) and **HL^{Mes}** (**3**) in a CH_3OH solution containing $Cu(CH_3COO)_2$ (Scheme 5).

A similar procedure was used for the synthesis of the Zn(II) complex, containing the **HL^{CF3}** (**1**) ligand, and for the synthesis of the Zn(II) complex, containing the **HL^{Mes}** ligand (**3**), obtaining the corresponding species $[Zn(L^{CF3})_2]$ (**9**), and $[Zn(L^{Mes})_2]$ (**15**). The elemental analyses have confirmed the stoichiometry of the complexes **7**, **9**, **14** and **15**, showing a good purity of the products. The IR spectra was carried out on solid samples of **7**, **9**, **14** and **15**. They show all the expected absorption bands; in particular, absorptions in the range 3356-2858 cm^{-1} due to the C-H bonds; medium absorptions in the range 1629-1533 cm^{-1}, due to the asymmetric stretching of the C=O groups; absorptions in the range 1564-1503 cm^{-1}, attributable to the C=C/C=N double bonds. The ligand coordination sites involved in bonding with the metal ions was determined by careful comparison of the infrared absorption bands of the complexes with those of the parent ligands **HL^{CF3}** and **HL^{Mes}**. The relevant changes were the following: a frequency shift (4-6 cm^{-1}) in the carbonyl vibration; shifts to lower frequencies (3-10 cm^{-1}) in the C-C stretching of the methyl group in-plane bending vibrations. All these shifts suggest coordination of the ligand as an enolate. The 3556-2858 cm^{-1} region of the spectra of all complexes shows broad bands, which may be due to lattice and/or coordinated water molecules associated with the complexes. The carbonyl stretching frequencies fall in a similar range and suggest little sensitivity to steric or electronic properties. These values are comparable with those reported in the literature for analogues Cu(II) complexes supported by bulky β-diketones [29, 30].

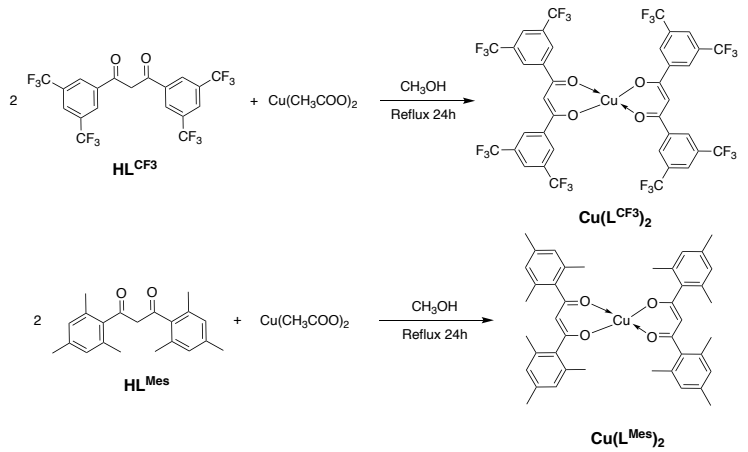

Scheme 5 - Synthetic procedure for the Cu(II) complexes of $Cu(L^{CF3})_2$ (**7**) and $Cu(L^{Mes})_2$ (**14**)

The Cu(I) complex $[Cu(PPh_3)_2(L^{CF3})]$ (**8**) was prepared from the reaction of PPh_3, $Cu(CH_3CN)_4PF_6$ and the sodium salt **NaL^{CF3}** (Scheme 6).

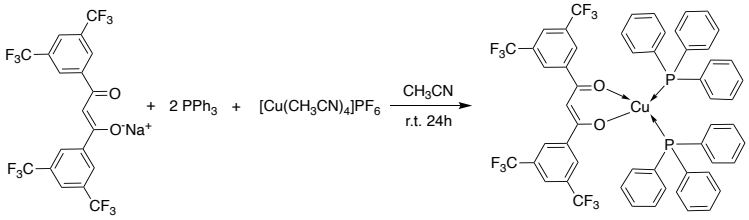

Scheme 6 - Synthesis of the complex $[Cu(PPh_3)_2(L^{CF3})]$ (**8**)

The IR spectrum carried out on a solid sample of **8** shows all the expected bands for the β-diketone ligand and the triphenylphosphine co-ligand. The absorptions due to the C=O stretching are at 1625-1581 cm^{-1}; they don't significantly vary with respect to the same absorptions of the carbonyl group detectable in the spectrum of the free ligand (1623-1576 cm^{-1}). The ^{1}H-NMR spectrum of the Cu(I) complex, recorded in $CDCl_3$ solution at room temperature, shows a single set of resonances for the β-diketone moiety, indicating that the protons of the aromatic rings are equivalents, with a slight shift due to the coordination to the metal center. The PPh_3 co-ligand shows a characteristic series of peaks in the range 7.22-7.42 ppm, with an integration, with respect to the ligand peaks, which confirms the 1:2 stoichiometric ratio between the β-diketone ligand and the phosphane co-ligand. The ^{31}P{H}-NMR spectrum at 223 K of **8** recorded in $CDCl_3$ solution at 223 K, gives a broad single signal at -3.683 ppm downfield shifted with respect to the value of the free phosphane (δ = -5.36 ppm). The ESI-MS study was performed by dissolving **8** in CH_3CN and recording the spectrum in positive-ion mode. The molecular structure of **8** was confirmed by the presence of the molecular peaks at *m/z* 366 and 586, attributable to the $[Cu(PPh_3) + CH_3CN]^+$ and $[(Cu(PPh_3)_2]^+$ species, being positive fragments of the dissociation of the ligand from the complex.

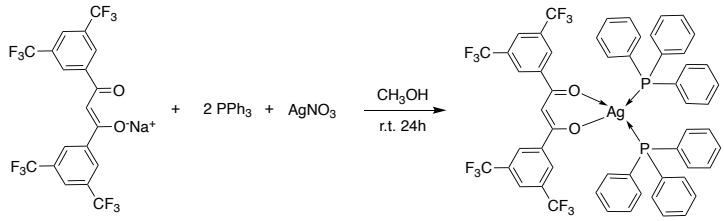

Scheme 7 - Synthesis of the complex $[Ag(PPh_3)_2(L^{CF3})]$ (**10**)

The Ag(I) complex $[Ag(PPh_3)_2(L^{CF3})]$ (**10**) was prepared from the reaction of PPh_3, $AgNO_3$ and the sodium salt **NaL^{CF3}** (Scheme 7).

The IR spectrum carried out on a solid sample of **10** shows all the expected bands for the β-diketone ligand and the triphenylphosphine co-ligand. The absorptions due to the C=O stretching are at 1626-1579 cm^{-1}; they don't significantly vary with respect to the same absorptions of the carbonyl group detectable in the spectrum of the free ligand. The ^{1}H-NMR spectrum of the Ag(I) complex **10**, recorded in $CDCl_3$ solution at room temperature, shows a single set of resonances for the β-diketone moiety, indicating that the protons of aromatic rings are equivalents, with a slight shift

due to the coordination to the metal center. The PPh_3 coligand shows a characteristic series of peaks at δ 7.29-7.46 ppm, with an integration, with respect to the ligand peaks, which confirms the 1:2 stoichiometric ratio between the β-diketone ligand and the phosphane co-ligand. The $^{31}P\{^1H\}$-NMR spectrum of **10** was recorded at 223 K in $CDCl_3$ solution. In the spectrum of **10** we observed a doublet of doublet centered at 9.64 ppm with coupling constants $J(^{107}Ag\text{-}^{31}P)$ = 432 and $J(^{109}Ag\text{-}^{31}P)$ = 499 Hz. These values have confirmed the coordination of two phosphanes to the metal centre; in addition, the ratio between these two coupling constants values is in accordance with the gyromagnetic ratio of silver.
The new β-diketone ligands **HL^J** and **HL^{JM}** having additional pyrazoles are really versatile N,O,O-donors because they can provide different hapticities, depending on the type of coordination environment of the metal (Fig.1).

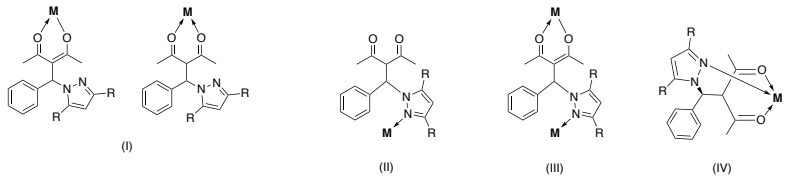

Figure 1 - Coordination modes of **L^J** and **L^{JM}** ligands (**L^J**: R = H; **L^{JM}**: R = Me)

Among the classic coordination modes of β-diketones, these ligands could be coordinated to metal ions in both neutral (keto) or mono-anionic (enol) form, as κ^2-O,O-chelating symmetrical or not-symmetrical donors (Figure 8 I). In addition, they could engage the nitrogen atom of the heterocycle acting as N-monodentate ligand (Figure 8 II) or engaging both the two oxygen atoms of the carbonyl groups and the nitrogen atom of the pyrazole moiety acting as N,O,O-bridging ligand (Figure 8 III). In the neutral keto-form they could be also coordinated in the κ^3-N,O,O-tridentate form typical of "scorpionates" (Figure 8 IV).
The copper(II) complex $[Cu(L^J)_2]$ (**11**) was synthesized in good yields by dissolving the corresponding ligand **HL^J** (**5**) in a CH_3OH solution containing the $Cu(CH_3COO)_2$ acceptor (Scheme 8).

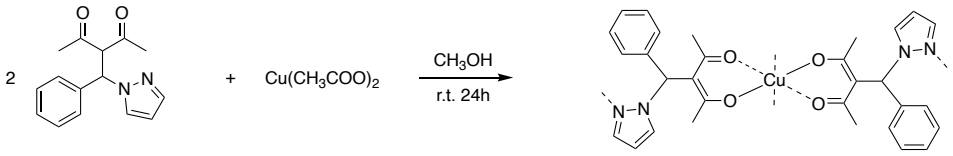

Scheme 8 - Synthetic procedure for the $Cu(L^J)_2$ complex (**11**)

A different procedure was used for the synthesis of the Zn(II) complexes, containing the **HL^J** ligand obtaining the corresponding species $Zn(HL^J)(HPz)Cl_2$ (**13**) (Scheme 9).

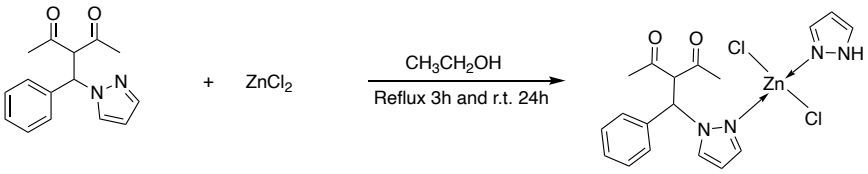

Scheme 9 - Synthetic procedure for the $Zn(HL^J)(HPz)Cl_2$ (**13**) complex

The elemental analyses have confirmed the stoichiometry of the complexes **11** and **13** showing a good purity of the products. The IR spectra were carried out on solid samples of **11** and **13**. They have shown all the expected absorption bands; in particular, absorptions in the range 3300-2916 cm^{-1} due to the C-H bonds; strong absorptions in the range 1732-1700 cm^{-1}, due to the asymmetric stretching of the C=O groups. The ligand coordination sites involved in bonding with the metal ions were determined by careful comparison of the infrared absorption bands of the complexes with those of the related ligands **HL^J**. The relevant changes were the following: a little shift to lower frequency in the energy carbonyl vibration; shifts to lower frequencies (6-15 cm^{-1}) in the C-C stretching of the methyl group in-plane bending vibrations. All these shifts could suggest coordination of the ligand in the keto form. The absorptions of carbonyl stretching vary little with respect to the same absorptions of the carbonyl group detectable in the spectrum of the free ligand (1732-1699 cm^{-1}), therefore a coordination involving the nitrogen of pyrazole in the ligand moiety is also plausible. In the ^1H-NMR spectrum, recorded in CD_3CN for complex **13**, the 3-C*H* and 4-C*H* protons of the pyrazole ring are present at 7.63 and 6.25 ppm, respectively. The 5-C*H* proton of the pyrazole and the C*H* aromatic protons of the phenyl ring are present in the range 7.35-7.49 ppm. The α-C*H* and γ-C*H* bridging protons are present at 5.47 ppm (^3J = 11.28 Hz) and 6.12 ppm (^3J = 11.28 Hz). The singlets at 2.18 and 2.06 ppm are attributable to the methyl groups bonded to the β-dicarbonyl moieties. The signal at 6.57 (4-C*H*), the broad doublet at 7.86 (3- and 5-C*H*) and the singlet at 11.69 (N*H*) show the presence of another pyrazole moiety in the complex. This pyrazole moiety is probably due to the

decomposition of the ligand in solution in these specific reaction conditions. Therefore, the low yield for the synthesis of **13** could confirm this assumption. The ESI-MS study was performed by dissolving complexes **11** and **13** in CH_3CN, recording the spectra in positive- and negative-ion mode. The molecular structure of **11** was confirmed by the presence of the molecular peaks at *m/z* 318 and 360 respectively, attributable to the $[Cu(L^J)]^+$ and $[Cu(L^J) + CH_3CN]^+$ species. The molecular structure of **13** has been confirmed by the presence of the molecular peaks at *m/z* 257, 279 and 355 respectively, attributable to the $[L^JH + H]^+$, $[Zn(L^J - Ph) +Cl)]^+$ and $[Zn(HL^J) + Cl]^+$ species. The ESI-MS spectrum of **13** in CH_3CN recorded in negative-ion mode shows peak at *m/z* 171 attributable to the $[2Pz + Cl^-]$ aggregate.
The Cu(I) complex $[Cu(PPh_3)_2(HL^J)]PF_6$ (**12**) was prepared from the reaction of PPh_3, $Cu(CH_3CN)_4PF_6$ and ligand **HL^J** in CH_3CN solution (Scheme 10).

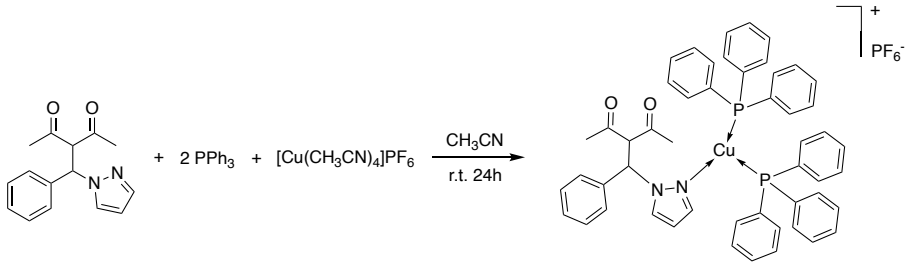

Scheme 10 - Synthesis of complex $[Cu(PPh_3)_2(HL^J)]PF_6$ (**12**)

The IR spectrum carried out on a solid sample of **12** shows all the expected bands for the β-diketone ligand and the triphenylphosphine coligand. The absorptions due to the C=O stretching are at 1731-1702 cm^{-1}; they don't significantly vary with respect to the same absorptions of the carbonyl group detectable in the spectrum of the free ligand (1732-1699 cm^{-1}). In a lower frequency region, complex **12** shows a broad strong band at 832 cm^{-1} due to the stretching vibrations of the PF_6^- anion. The $\delta(PF_6)$ bending vibrations in the spectra of all hexafluorophosphate complexes are observed as a narrow strong band at 556 cm^{-1}. In the ^{1}H-NMR spectra of **12**, recorded in $CDCl_3$ solution at room temperature, the 3-C*H* and 4-C*H* protons of the pyrazole ring are present at 7.68 and 6.27 ppm, respectively. The 5-C*H* proton of the pyrazole ring and the C*H* aromatic protons of the phenyl rings are present in the range 7.13-7.43 ppm. The α–C*H* and γ–C*H* bridging protons are present at 5.58 ppm (^3J = 11.28 Hz) and 6.17 ppm (^3J = 11.28 Hz). The singlets at 2.14 and 2.06 ppm are attributable to the methyl groups bonded to the β-dicarbonyl moieties. The ^{31}P{H}-NMR spectrum of the Cu(I) complex **12**, recorded in $CDCl_3$ solution at room temperature, gave a broad singlet at -0.86 ppm downfield shifted with respect to the value of the free phosphane (δ = -5.36 ppm). In the spectrum the characteristic septet centered at -144.21 ppm is due to the PF_6^- counterion. The ESI-MS study was performed by dissolving **12** in CH_3CN and recording the spectra in positive- and negative-ion mode. The molecular structure of **12** was confirmed by the presence of the peaks at *m/z* 366 and 587, attributable to the $[(Cu(PPh_3) + CH_3CN]^+$ and $[(Cu(PPh_3)_2]^+$ species, being positive fragments of the dissociation of the ligand from the complex. The ESI-MS spectrum of **12** in CH_3CN recorded in negative-ion mode shows peak at *m/z* 145 attributable to the PF_6^- aggregate, confirming the presence of the counterion (PF_6^-).

4. Crystallographic structures

Slow evaporation of a hexane solution of **HL^J** afforded a batch of good quality crystals, from which a specimen of 0.60 × 0.38 × 0.22 mm was selected for the X-ray work. The X-ray crystallographic analysis of **HL^J** was performed by Prof. Alessandro Dolmella of Department of Pharmaceutical and Pharmacological Sciences, University of Padova, using a kappa-geometry Oxford Diffraction Gemini EOS diffractometer, equipped with a 2K × 2K CCD area detector and sealed–tube Enhance (Mo) and (Cu) X-ray sources. The crystallographic investigation revealed the solid-state molecular structure of the ligand **HL^J** (**5**). An ORTEP drawing of the ligand is shown in Fig. 2 a) e b).
The ligand shows two almost perfectly planar pyrazolyl and phenyl rings. The C(8)-O(1) and C(6)-O(2) bonds of 1.194(2) and 1.194(2) Å has instead a clear double bond character. Notably, the two carbonyl C=O moieties are in the cis conformation. Among the two methyl groups, only one has intermolecular O(1)-H(7C) interactions with the carbonyl group of a second molecule present in the same cell unit (Fig. 2 c)). A complete list of bond distances and angles is given in Table 1.

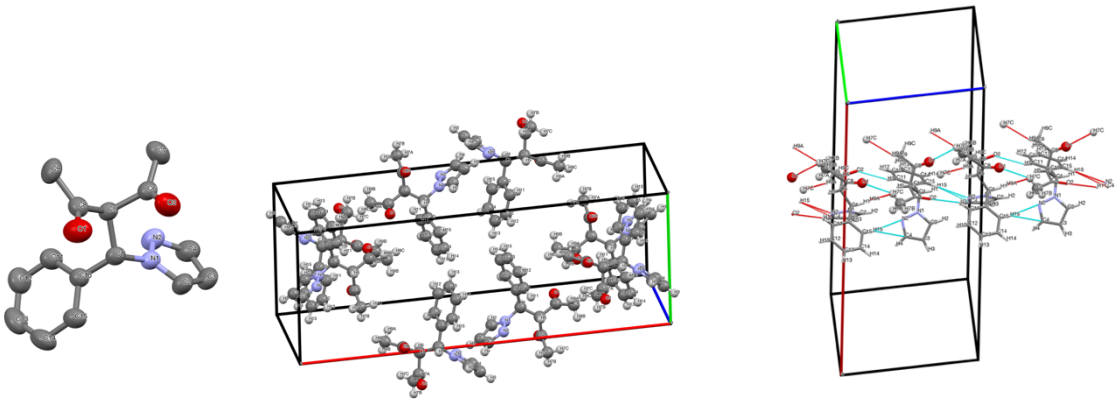

(a) (b) (c)

Figure 2. a) ORTEP view of **HL^J** (**5**) with thermal ellipsoids drawn at the 30% probability level. Hydrogen atoms have been omitted. b) Packing structure view of **HL^J**. c) Nonbonding interactions in **HL^J**.

Table 1 - Bond lenghts (Å) and angles (°) for compound **HL^J**.

Bond lenghts (Å)

O1-C8	1.194(2)	C5-C6	1.537(2)
O2-C6	1.1959(19)	C5-C8	1.532(2)
N1-N2	1.3405(18)	C6-C7	1.479(3)
N1-C1	1.4694(19)	C8-C9	1.489(3)
N1-C2	1.338(2)	C10-C11	1.379(2)
N2-C4	1.333(2)	C10-C15	1.383(2)
C1-C5	1.531(2)	C11-C12	1.385(3)
C1-C10	1.519(2)	C12-C13	1.366(3)
C2-C3	1.358(3)	C13-C14	1.364(3)
C3-C4	1.370(3)	C14-C15	1.389(3)

Angles (°)

N2-N1-C1	120.54(12)	O2-C6-C7	122.94(16)
C2-N1-N2	112.19(14)	C7-C6-C5	116.90(15)
C2-N1-C1	127.27(14)	O1-C8-C5	120.37(14)
C4-N2-N1	103.66(14)	O1-C8-C9	123.12(17)
N1-C1-C5	109.98(12)	C9-C8-C5	116.46(16)
N1-C1-C10	110.71(12)	C11-C10-C1	123.05(14)
C10-C1-C5	114.08(12)	C11-C10-C15	118.44(16)
N1-C2-C3	107.09(17)	C15-C10-C1	118.48(14)
C2-C3-C4	104.79(16)	C10-C11-C12	120.59(18)
N2-C4-C3	112.27(17)	C13-C12-C11	120.5(2)
C1-C5-C6	110.76(12)	C14-C13-C12	119.7(2)
C1-C5-C8	110.34(13)	C13-C14-C15	120.4(2)
C8-C5-C6	107.38(12)	C10-C15-C14	120.42(19)
O2-C6-C5	120.14(15)		

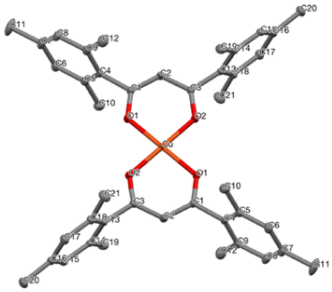

Figure 3 - ORTEP view of [Cu(L^{Mes})$_2$] complex (**14**) with thermal ellipsoids drawn at the 30% probability level. Hydrogen atoms have been omitted.

Slow evaporation of a chloroform/hexane solution of [Cu(L^{Mes})$_2$] (**14**) complex afforded a batch of good quality crystals useful for the X-ray work. The X-ray crystallographic analysis was performed by Prof. Rasika Dias of Department of Chemistry and Biochemistry, The University of Texas at Arlington, USA. The crystallographic investigation revealed the solid-state molecular structure of the [Cu(L^{Mes})$_2$] complex. An ORTEP drawing of complex (**14**) is shown in Fig.3. The neutral complex Cu(L^{Mes})$_2$ shows a stoichiometric ratio of 1:2 between the metal and the ligand, with the Cu(II) center chelated by four oxygen atoms of two deprotonated L^{Mes} ligands in the enolic form. The two chelated rings Cu-O(1)-C(1)-C(2)-C(3)-O(2) are almost perfectly coplanar and symmetrical with respect to the metal center. A selected list of bond distances and angles is given in Table 2.

Table 2 - Selected bond lenghts (Å) and angles (°) for compound Cu(L^{Mes})$_2$

Bond lenghts (Å)

Cu-O1	1.9166(9)
Cu-O2	1.9071(9)
O1-C1	1.2763(15)
O2-C3	1.2768(15)
C1-C2	1.3973(18)
C2-C3	1.3967(17)

Angles (°)

O1-Cu-O1	180.0
O2-Cu-O1	93.67(4)
O2-Cu-O1	86.33(4)
O2-Cu-O2	180.0
C1-O1-Cu	125.70(8)
C3-O2-Cu	125.98(8)
O1-C1-C2	125.33(12)
C3-C2-C1	123.88(12)
O2-C3-C2	125.28(12)

Copper(II) β-diketonates have a particularly regular structure across dozens of crystallographic examples [31]. Complexes exhibit nearly identical, coplanar chelate rings irrespective from steric or electronic properties of substituents.Among the four known complexes $Cu(L^{Me})_2$ [32], $Cu(L^{Me,Ph})_2$ [33], $Cu(L^{Ph})_2$ [34] e $Cu(L^{tBu})_2$ [35], the $Cu(L^{Me})_2$ complex has the longest Cu-O bonds, while $Cu(L^{tBu})_2$ has the shortest, on average (Table 3). This length also decreases as the methyl groups are exchanged for phenyl, as indicated by $Cu(L^{Me,Ph})_2$ and $Cu(L^{Ph})_2$. Another trend with substitution can be found in the chelate fold angles, decreasing similarly. The C–C and C–O bond lengths are indifferent to substitution, although $Cu(L^{Ph})_2$ has a notable difference between its C–O bonds because the aryl substituents enjoy conjugation to the diketonate. In the case of $Cu(L^{Me,Ph})_2$ and $Cu(L^{Ph})_2$ a coplanar arrangement of the aryl and chelate rings is preferred to enjoy conjugation; however, the phenyl groups show a slight deviation from coplanarity. All four complexes are square planar. The chelate rings are highly symmetric, with many pairs of bond lengths within experimental error of each other.

Table 3 - Selected bond angles and lengths as determined from X-ray crystallography for new and common complexes

Bond lengths (Å) 				**Angles (°)**	
Complex	M–O	C–O	C–C	O-Cu-O	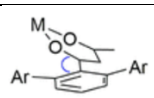 Aryl-chelate dihedral
$Cu(L^{Me})_2$	1.9268(16), 1.9227(16)	1.276(3), 1.275(3)	1.403(3), 1.402(3)	93.75(7)	
$Cu(L^{Me,Ph})_2$	1.924(3), 1.918(3)	1.270(5), 1.269(5)	1.400(6), 1.405(6)	93.16(13)	14.79
$Cu(L^{Ph})_2$	1.907(4), 1.910(5)	1.285(3), 1.260(2)	1.397(3), 1.393(4)	93.30(13)	10.56
$Cu(L^{tBu})_2$	1.902(2), 1.891(2)	1.273(3), 1.276(4)	1.376(5), 1.395(5)	92.80(10)	
$Cu(L^{Mes})_2$	1.9071(9), 1.9166(9)	1.2763(15), 1.27668(15)	1.3973(18)	93.67(4), 86.33(4)	89.92

Unlike the other aryl-substituted complexes, the $Cu(L^{Mes})_2$ complex (**14**) shows a dihedral angle between the aromatic rings and the chelated ring of 89.92º, indicating an almost complete absence of conjugation between the aromatic and β-diketone rings. This rare behavior, peculiar to the mesitylene groups, can be attributed to their high steric demanding.

5. Conclusions

The research project was mainly focused in the synthesis of first-row metal complexes of sterically hindered β-diketonates also bearing fluorinated moieties (**HL^{Mes}** and **HL^{CF3}**), with a particular attention to the Cu(II) and Cu(I) species, also in view of their catalytic and biological properties. Notably, **$Cu(L^{Mes})_2$** complex was fully characterized by X-ray crystallographic analysis in order to define its solid-state molecular structure. Additionally, preliminary X-ray crystallographic data of **$Cu(L^{CF3})_2$**, **$Cu(PPh_3)_2(L^{CF3})$** and **$Zn(L^{Mes})_2$** complexes were obtained. Furthermore, the modification of the electronic and steric properties of acetylacetonate was examined by insertion of different substituents in 2-position, containing additional donor atoms, in order to prepare polyfunctional coordinating ligands with higher complexity and functionality, and related metal complexes, in view of their biological activity as potential anticancer and antiviral agents. In particular, the 3-(phenyl(1*H*-pyrazol-1-yl)methyl)pentane-2,4-dione (**HL^{J}**) and the 3-((3,5-dimethyl-1*H*-pyrazol-1-yl)(phenyl)methyl)pentane-2,4-dione (**HL^{JM}**) have been synthesized; they are novel 1,3-diketones bearing a pyrazole moieties, whose reactivity and structure were fully studied also by X-ray diffraction analysis for **HL^{J}**. The new ligands (**HL^{J}** and **HL^{JM}**) are really versatile N,O,O-donors because they can provide different hapticities, depending on the type of coordination environment the metal is surrounded. The free ligands and the metal complexes have been fully spectroscopically and analytically characterized by elemental analysis, FT-IR, ESI-MS(+/-), ^{1}H-, ^{13}C-, ^{19}F- and ^{31}P-NMR. Biological studies to evaluate the antitumor and antiviral activity are in progress for some of the ligands and related metal complexes. Moreover, based on the scientific literature, they could have potential applications both in catalysis and in medicinal chemistry. For these reasons, the research work is worthy of further and deeper investigations of the properties of this class of compounds, as well as of the synthesis of novel analogous ligands and related complexes.

Acknowledgements

First of all, I would like to thank Prof. Maura Pellei and Prof. Carlo Santini for their infinite availability, for their indispensable advice and above all for their great organization and dedication to work which have been essential to grow professionally and personally. I thank Dr. Miriam Caviglia, who in these months of work has supported me with

great practical suggestions in laboratory research and in writing the thesis. I also thank Prof. Rasika Dias (University of Texas at Arlington, USA) and Prof. Alessandro Dolmella (University of Padova) for the X-ray crystallographic analysis. I would like to thank Prof. Luísa Margarida Martins who kindly accepted to be my supervisor. Finally, I would like to mention the importance of the Double Degree period in Lisbon, undertaken initially with absolute uncertainty and as a challenge, but which proved to be one of the experiences that allowed me to grow a lot not only at an educational level, but also at a human level.

References

[1] S. Ivanova, T.M. Martínez, Catalysts, 10 (2020) 247.
[2] P. Chirik, R. Morris, Acc. Chem. Res., 48 (2015) 2495.
[3] J.R. Ludwig, C.S. Schindler, Chem, 2 (2017) 313.
[4] C.C.C. Johansson Seechurn, M.O. Kitching, T.J. Colacot, V. Snieckus, Angew. Chem., Int. Ed., 51 (2012) 5062.
[5] R.M. Izatt, Metal Sustainability: Global Challenges, Consequences, and Prospects, 2016.
[6] J.M. Dennis, N.A. White, R.Y. Liu, S.L. Buchwald, J. Am. Chem. Soc., 140 (2018) 4721.
[7] D. Zhang, Q. Wang, Coord. Chem. Rev., 286 (2015) 1.
[8] S. Diez-Gonzalez, N-Heterocyclic Carbenes: From Laboratory Curiosities to Efficient Synthetic Tools, 2nd ed., The Royal Society of Chemistry, 2017.
[9] R.H. Crabtree, J. Organomet. Chem., 690 (2005) 5451.
[10] J.D. Hayler, D.K. Leahy, E.M. Simmons, Organometallics, 38 (2019) 36.
[11] D.C. Blakemore, L. Castro, I. Churcher, D.C. Rees, A.W. Thomas, D.M. Wilson, A. Wood, Nat. Chem., 10 (2018) 383.
[12] S.M. Krajewski, A.S. Crossman, E.S. Akturk, T. Suhrbier, S.J. Scappaticci, M.W. Staab, M.P. Marshak, Dalton Trans., 48 (2019) 10714.
[13] A.S. Crossman, M.P. Marshak, β-Diketones: Coordination and Application, in: Comprehensive Coordination Chemistry III, Elsevier, 2021, pp. 331.
[14] R.C. Mehrotra, 60 (1988) 1349.
[15] S. Kawaguchi, Coord. Chem. Rev., 70 (1986) 51.
[16] D.J. Bray, J.K. Clegg, L.F. Lindoy, D. Schilter, in: K. Eldik van R. Bowman-James (Ed.) Adv. Inorg. Chem., 2006.
[17] J. Emsley, N.J. Freeman, J. Mol. Struct., 161 (1987) 193.
[18] K.H. Hopmann, N.F. Stuurman, A. Muller, J. Conradie, Organometallics, 29 (2010) 2446.
[19] P.A. Vigato, V. Peruzzo, S. Tamburini, Coord. Chem. Rev., 253 (2009) 1099.
[20] V.W.-W. Yam, K.K.-W. Lo, Coord. Chem. Rev., 184 (1999) 157.
[21] G.L. Abbati, A. Cornia, A.C. Fabretti, A. Caneschi, D. Gatteschi, Inorg. Chem., 37 (1998) 1430.
[22] A.M. Fatta, R.L. Lintved, Inorg. Chem., 10 (1971) 478.
[23] H. Masui, Coord. Chem. Rev., 219-221 (2001) 957.
[24] E. Buck, Z.J. Song, D. Tschaen, P.G. Dormer, R.P. Volante, P.J. Reider, Org. Lett., 4 (2002) 1623.
[25] N.S. Nandurkar, M.J. Bhanushali, D.S. Patil, B.M. Bhanage, Synth. Commun., 37 (2007) 4111.
[26] K. Kumpan, A. Nathubhai, C. Zhang, P.J. Wood, M.D. Lloyd, A.S. Thompson, T. Haikarainen, L. Lehtiö, M.D. Threadgill, Bioorg. Med. Chem., 23 (2015) 3013.
[27] C. Zhang, P. Yang, Y. Yang, X. Huang, X.-J. Yang, B. Wu, Synth. Commun., 38 (2008) 2349.
[28] R.C. Fuson, W.E. Ross, C.H. McKeever, J. Am. Chem. Soc., 61 (1939) 414.
[29] A.T. Larson, A.S. Crossman, S.M. Krajewski, M.P. Marshak, Inorg. Chem., 59 (2020) 423.
[30] C. He, G. Zhang, J. Ke, H. Zhang, J.T. Miller, A.J. Kropf, A. Lei, J. Am. Chem. Soc., 135 (2013) 488.
[31] S.A. Gromilov, I.A. Baidina, J. Struct. Chem., 45 (2004) 1031.
[32] P.C. Lebrun, W.D. Lyon, H.A. Kuska, J. Crystallogr. Spectrosc. Res., 16 (1986) 889.
[33] S.K. Dey, B. Bag, Z. Zhou, A.S.C. Chan, S. Mitra, Inorg. Chim. Acta, 357 (2004) 1991.
[34] Z.A. Starikova, E.A. Shugam, J. Struct. Chem., 10 (1969) 267.
[35] S. Sans-Lenain, A. Gleizes, Inorg. Chim. Acta, 211 (1993) 67.